Intrinsic low-temperature thermal properties of glasses*

Richard B. Stephens[†]

Laboratory of Atomic and Solid State Physics and Materials Science Center, Cornell University, Ithaca, New York 14853

(Received 15 July 1975)

The well-known specific-heat anomaly in amorphous dielectrics and their universal thermal conductivity have been carefully studied for the same wide variety of glasses as reported previously. The present studies have shown that the thermal conductivity is entirely insensitive to variations of the chemical purity or the thermal history of the samples. In contrast, the excess specific heat is sample dependent. In some materials, it is reduced by a factor of 2 by careful preparation. However, it has not been found to scale with any known impurity and is still present in the most carefully prepared and purest samples. There is a correlation between the remaining excess heat capacity and the thermal conductivity, but assuming them to be caused by the same centers requires a very strong scatterer compared to previously observed defect centers in crystals. These observations indicate that the connection between the specific-heat anomaly and the thermal conductivity, i.e., the phonon scattering, is more complex than has previously been assumed. Preliminary measurements on a chemically complex, crystallized glass ceramic, pyroceram, were also preformed. It showed the same thermal characteristics as the homogenous glasses. Hence, it appears that the disorder required to produce these "glassy" properties is not incompatible with a substantial amount of atomic order.

I. INTRODUCTION

Recent measurements[1-12] have demonstrated that the low-temperature thermal properties of non-crystalline dielectric solids are markedly different from those observed in crystalline materials: (i) The heat capacities are considerably larger than those predicted by the Debye model (which works very well for crystalline materials), and most can be described by the equation

$$C = c_1 T + c_3 T^3 , \qquad (1)$$

where c_1 is 5–50 erg gK^2, and $c_3 > c_{Deb}$. (ii) They also have very similar thermal conductivities. Below 1 K, they can be described by a power law of the form

$$\Lambda = \beta T^\delta , \qquad (2)$$

where T is in °K, $\delta = 1.9 \pm 0.1$, and $\beta = 10^{-3} - 10^{-4}$ W/cm K.

These phenomena appeared to be quite general among amorphous materials, and the present work was started to explore the limits of their applicability. The problem was approached in two ways. First, the possibility of impurity effects in the previous measurements was checked with samples which contained fewer or different impurities. Second, the range of these "glassy" properties was investigated by looking at a more complex material: a polycrystalline material, which has a long-range structural disorder, but which for short lengths ($d < 600$ Å) is crystalline by any standard measure.

II. EXPERIMENTAL TECHNIQUES

Specific heat and thermal conductivity were measured in the temperature range 0.05–4 K in the adiabatic demagnetization cryostat, and with the techniques described by Harrison[13] and used for earlier work.[9-12] The procedure for processing and recording heat-capacity data has been partially automated by mechanically interfacing Harrison's resistance bridge with a data-recording system. This add-on approach was much simpler and more economical than building from scratch one of the previously described systems.[14]

A simple schematic of the finished system is shown in Fig. 1. One can see that the data-recording system is largely independent of the detailed construction of the resistance bridge; since there are no electrical connections, they can not interfere with one another.

In addition, the system is very simple to operate. All of the timing intervals are internally determined. The length of the heat pulse is set to 1.38 sec by a monostable flip-flop which consists of a C.P. Clare bistable high-speed Hg relay driven by a Signetics NE555V IC timer. The pulse length produced by this circuit is only slightly dependent on its duty cycle; in practice the reproducibility of the pulse length is limited to 0.1% by nonuniformities in the relay movements.

One records the change in the sample temperature as a function of time after the heat pulse directly on a strip-chart recorder in the form $\ln\Delta R(t)$ vs t [$\Delta R(t)$ is the change in the resistance of the sample thermometer at time t after the heat pulse]. The times at which the bridge is balanced are indicated on the chart by a manually actuated event marker. The bridge settings $\Delta R(t)$ are sensed by a General Radio decade resistance box which is coupled to an identical box in the bridge circuit which is used to rebalance the bridge after the heat pulse. A constant current I_c flows through the slaved box and produces a voltage across it pro-
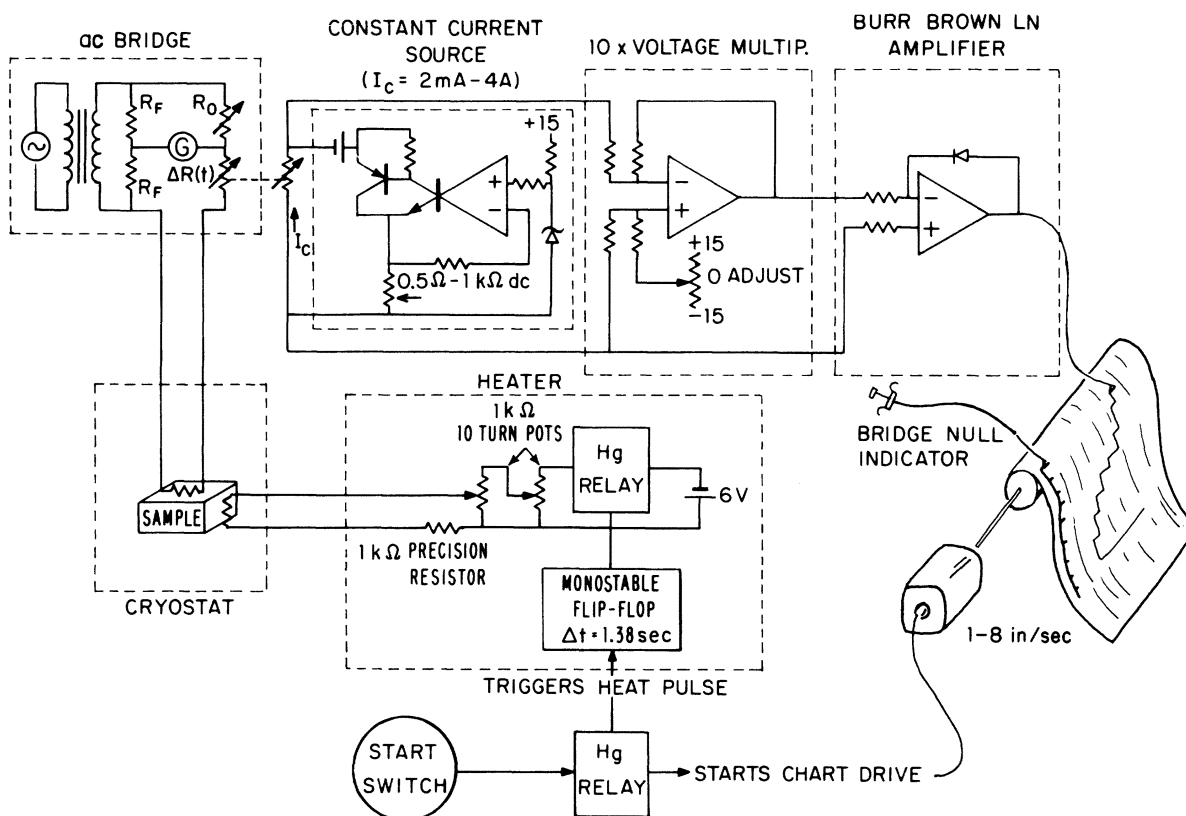
FIG. 1. Simplified schematic of the semiautomated system for recording heat-capacity data. For a discussion of the components, see text.

portional to $\Delta R(t)$. Because the decade box cannot dissipate very much power, this voltage is rather small (<1 V), so it is multiplied 10 times before going to a Burr Brown Logarithmic Amplifier (Model 1674/16). The amplifier produces a logarithmic output ($\pm 1\%$) for three decades of input voltage (0.1–10 V). This range is more than adequate to plot $\Delta R(t)$ for a single heat pulse. The $\Delta R(0)$'s, however, have quite a large range (<1 Ω at 2 K to 5 kΩ at 0.06 K); to accomodate the wide span which they encompass, a switch bank was incorporated enabling I_c to be stepped by factors of 5 from 2 mA to 4 A.

This system is also quite easy to maintain. The only adjustment which is critical is the zero adjustment in the 10× multiplier. For an accurate log output is is necessary to balance out the constant lead voltage V_L from the resistance box lead resistance. Since V_L is proportional to I_c, the zero adjustment must be changed every time I_c is changed.

A typical heat-pulse record is shown in Fig. 2. It is produced in several steps. Before the heat pulse, one marks a span of one decade in the paper (500 and 50 Ω in this example); one of the points should be near the estimated $\Delta R(0)$. Then one

starts the heat pulse and records $\ln\Delta R(t)$ vs t on the chart (the heavy lines in Fig. 2). When one has finished measuring, one combines the marks from the event marker, and the stepped trace from the log amplifier to get a set of data points. If the cryostat temperature were stable and there were no extraneous heat inputs to the sample, the points
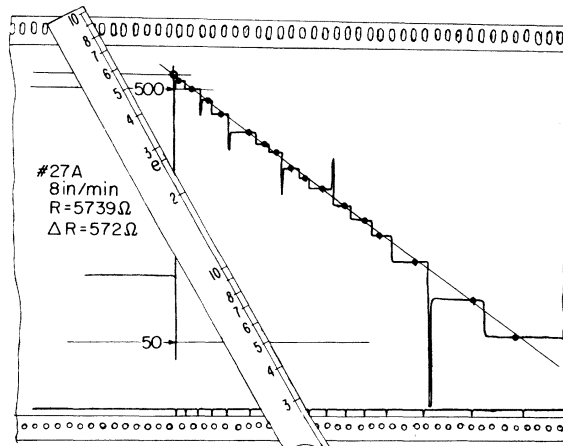
FIG. 2. Typical heat-pulse record and analysis. For an explanation see text.

will lie on a straight line and one can easily extrapolate back to $t = 0$. One now determines $\Delta R(0)$ using the two-decade marks, and a two-decade logarithmic ruler (this can be made out of logarithmic graph paper). The ruler is tilted to fit the decade marks; one can then read off $\Delta R(0)$ to $\sim 2\%$. There is another 2% uncertainty in the heat pulse owing to random heat inputs (this uncertainty is somewhat larger at the lowest temperatures), so the final heat capacity has an uncertainty of $\lesssim 5\%$.

In order to determine the Debye contribution to the specific heat and to calculate phonon mean free paths, it is necessary to know the speed of sound in each glass. Fortunately this was already known for all of the samples except the following three: $3SiO_2 \cdot Na_2O$, $CaK(NO_3)_3$, and Corning's Pyroceram. Measurements were made of the velocity of propagation of longitudinally and transversely polarized 10-MHz sound waves in these samples. A single-ended pulse-echo technique was used. The samples were cut 1–2 cm long and 1 cm in diameter. The ends were polished flat and parallel to within a few wavelengths of visible light; this is a very good optical polish for the acoustic-phonon wavelength of 0.05 cm. Using the calibrated time-delay feature of an oscilloscope, the echo times could be determined to 0.1%. Since the measurement was performed at 4.2 K the accuracy of the calculated velocities are limited to 1% by uncertainty in the thermal contraction. The measured velocities are shown in Table I.

III. NONCRYSTALLINE SOLIDS

A. Specific heat

It was noted in the previous paper[10] that the samples used for that study were certainly not pure enough to rule out an extrinsic cause for these thermal characteristics. However, the apparent universality and uniformity of these characteristics led to the suggestion that the effects were intrinsic. In the present study, that assumption was checked more rigorously. Purer or differently prepared samples were obtained of several of the materials which had been previously measured—SiO_2, $CaK(NO_3)_3$, B_2O_3, and As_2S_3—and their specific heat and thermal conductivity were measured and compared with earlier measurements.

As before, C_{exp} was found to be considerably larger than C_{Deb} in all the glasses measured. However, the size of the excess was also found to be sample dependent. The first conclusion one might draw is that these variations, and perhaps all of the excess in the heat capacities, must be caused by chemical impurities. Indeed, that could very easily happen; the number of modes contributing to the Debye heat capacity in this low-temperature range is very small (0.1% of the total number of modes at 0.5 K for silica), and it would not take very many extrinsic excitations to drastically increase the observed heat capacity. It was calculated that only 10 systems per million atoms, ppma, with the appropriate low-frequency excitations could cause the observed excess in the heat capacity.[10]

Commercial borosilicate glasses illustrate this point well. They have a large anomaly in heat capacity at ~ 3 K caused by the presence of iron (Fig. 1). That the variation in the borosilicate glasses' heat capacity is due to unpaired electrons in the Fe ions can be shown by observing that the excess heat capacity scales with the Fe impurity concentration, and that a large magnetic field removes the excess altogether out of the measured temperature range; the magnetic field increases electron-spin level splittings, $\Delta E = g\mu_B H$, and this shifts the specific-heat anomaly to high temperatures. The remaining heat capacity is similar to that of other glasses like, for instance, the soda-silica glass which is also graphed in Fig. 3.

It is, however, not nearly so clear that the excess heat capacity remaining in a high magnetic field in the borosilicate glasses and the excesses found in all the other glasses can be due to chemical impurities. In the first place, the probability is quite low that a given impurity will add to the heat capacity of its host. In crystalline alkali halides, for instance, Narayanamurti and Pohl[15] have shown that ionic impurities contribute to the low-temperature heat capacity in a very limited number of situations. The Li^+ ion, for example, produces a specific-heat anomaly in KCl, but not in KBr or NaBr.[15] In the second place, the heat capacities seen in the glasses studied here do not scale with impurity concentrations. To demonstrate this, it is necessary to review the glasses individually.

TABLE I. Speed of sound in $Na_2O \cdot 3SiO_2$, $CaK(NO_3)_3$, and Pryoceram. The measurements were made with a 10-MHz quartz transducer at 4 K, and the speeds were calculated using the room-temperature sample length. The average speed, $v_{Deb} \equiv (1/3v_l^3 + 2/3v_t^3)^{-1/3}$, was decreased by 1% to account for thermal contraction in cooling to 4 K. v_{Deb} is shown for all the glasses used in this study in Table V column 4.

Material	Sample length (cm)	v_l	v_t	v_{Deb}
		(10^5 cm/sec)		
$Na_2O \cdot 3SiO_2$	2.380	5.370	3.199	3.51
$CaK(NO_3)_3$ "dry"	0.710	3.456	1.749	1.94
Pyroceram	1.959	6.170	3.766	4.12

FIG. 3. Specific heat of Corning borosilicate glasses code No. 7740 and No. 9700. The No. 7740 data ($\triangle$) are after Zeller and Pohl (Ref. 10); the No. 9700 data were made in both 0-kG ($\blacktriangle$) and 33-kG ($\bullet$) magnetic fields. Data from a soda-silican glass ($3SiO_2 \cdot Na_2O$) are included (O) for comparison to the borosilicate's 33-kG heat capacity. The sizes of the anomaly are roughly that expected from the measured concentration of iron in these glasses: 100 ppm for No. 7740, and 12 ppm for No. 9700 (Ref. 12).

1. SiO$_2$

The first sample measured below 1 K (Zeller and Pohl[11]) was a silica (Spectrosil, from the Thermal American Fused Quartz Co.), made by cracking silane gas. For this work a fused quartz (Vitreosil, also from Thermal American), which is made by melting quartz crystals was measured. The different methods of production of the samples result in strikingly different nominal impurity levels in the two samples, as shown in Table II.[16]

Several samples obtained from a variety of other

TABLE II. Impurities in amorphous SiO$_2$ produced by two different methods: melting quartz crystals (fused quartz), and cracking silane (silica).

	OH	Metals (mostly Al)
Silica	0.1 wt%	0.1 ppm
Fused quartz	0.0003 wt%	50 ppm
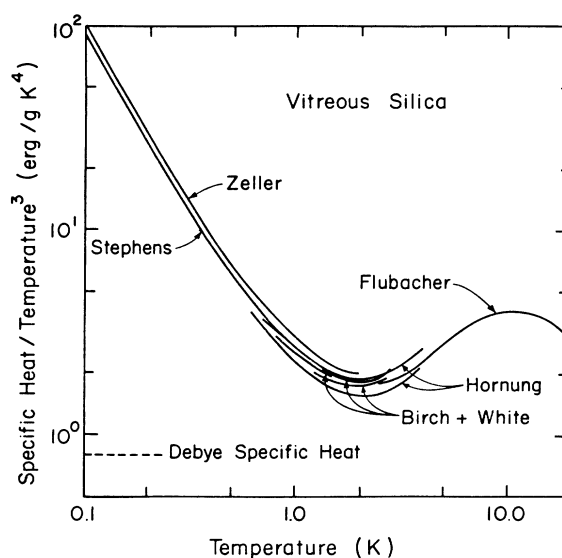
FIG. 4. Comparison of the specific heat of eight samples of SiO$_2$ measured by different experimenters, presented at C/T^3 vs T. Zeller and Pohl (Ref. 10) measured a sample of vitreous silica. White and Birch (Refs. 17 and 18) and this work made measurements on samples of fused quartz. Flubacher (Ref. 19) and Hornung (Ref. 20) did not specify which variety of SiO$_2$ they used. The dashed line at the bottom of the graph is the heat capacity predicted by the Debye model.

companies have been measured in the neighborhood of 1 K by other experimenters (Birch and White[17,18] used IR Vitreosil from Thermal Syndicate Ltd., and Flubacher[19] and Hornung[20] used SiO$_2$ from the Amersil Div. of Engelhard Ind.), but all were produced by one of the two processes listed above, and so have impurities corresponding to one of the categories in Table II. Lasjaunias et al.[7] have recently measured a sample of SiO$_2$ which was treated to remove OH. It contained ~ 1.5 ppm OH, ~ 0.5 ppm metal ions, and 200 ppm each Cl and F. This sample has a slightly lower heat capacity than those previously measured. At 0.1 K the difference is ~ 15%, and at 0.025 K (their lowest temperature) it is ~ 40%.

The heat capacities of these samples are shown in Fig. 4. There is some scatter between the different measurements, but when one considers the orders of magnitude differences in net and individual impurity concentration between the several samples, it is readily apparent that only a small fraction of the heat capacity of this material could be caused by impurities.

2. CaK(NO$_3$)$_3$

CaK(NO$_3$)$_3$ samples were produced with a range in water concentrations of over 10^3. The samples
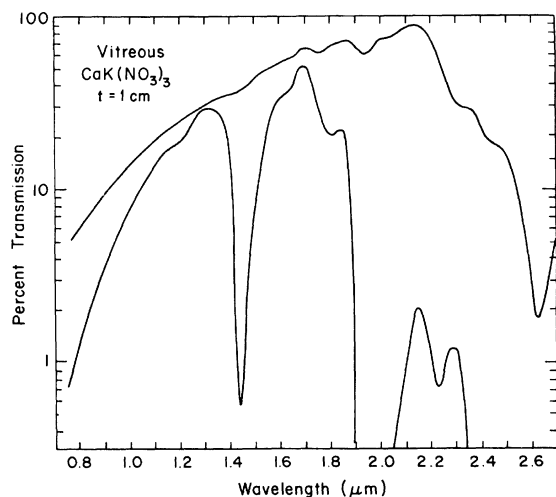
FIG. 5. Infrared absorption spectra of $CaK(NO_3)_3$ sample Nos. 1 and 3. The results are normalized to % transmission for a sample thickness t of 1 cm. The top line is for the "dry" sample (No. 3), and the lower one is for a "wet" sample (No. 1). The rapid fall-off of transmission at the high-frequency end of the wet sample spectrum is due to scattering from the poor sample surfaces, reflecting the difficulty of polishing such a soft material.

were produced in Cornell's Crystal Growing Facility from equimolar amounts of AR-grade KNO_3 and $Ca(NO_3)_2 \cdot 4H_2O$. It was then heated until the mixture dissolved into its own water of hydration and the water boiled off. For the previous paper,[10] two separate samples (Nos. 1 and 2) were made by driving off just enough water that the samples would solidify when they were cooled. The large amounts of water contained in these "wet" samples was easily seen in the ir absorption spectrum (Fig. 5). For the present study a "dry" sample (No. 3) was prepared by increasing the boiling time (see the previous paper[10]). You can see from Fig. 3 that the H_2O absorption lines are very weak for this sample; the difference is roughly a factor of 10^3. However, you can also see in Fig. 6 that there is only a 30% difference in the heat capacity of these samples.

In this instance, the impurity concentration differed so much in the two glasses that it was questionable whether it was valid to compare them. The wet samples contained so much water that they were plastic (you could push a pencil point into them), while the dry sample was very brittle. Thus this small change in specific heat may well be due to a basic difference in structure between the hydrated and unhydrated glass, as indicated by their sharply differing hardness. It proved impossible to relate this difference to a change in sound velocity; the wet samples were far too soft to prepare for an ultrasonics experiment.

3. B_2O_3

Like $CaK(NO_3)_3$, B_2O_3 is hygroscopic, and water absorption lines were also detected in these samples (see Fig. 7). However, the absorption lines were not nearly as strong in the B_2O_3 perhaps because of the higher melt temperatures made possible by its higher boiling temperature. The starting material contained enough water that it had to be dehydrated overnight in a vacuum furnace at 200 °C. The caked powder was then broken up and transferred into a platinum crucible. The first sample (No. 1; see Table III) was heated to 670 °C for 1 day; the next two samples (Nos. 2 and 3) were heated to 1050 °C for 3 days. They were slowly cooled by turning off the oven. In order to dehydrate No. 3 further, it was transferred to a crystal-growing furnace and heated in vacuum to 1250 °C for 2 h (at this point about half the sample had boiled away), and then slowly cooled.

Lasjaunias's two samples (Nos. 4 and 5) were prepared in a different way.[4,5] They were heated to a maximum of 1300 °C in air, and dry argon was bubbled through the melts for 3 and 4 h, respectively.

There was some variation in the heat capacity of these samples (Fig. 8 and Table III). The least pure sample (No. 1) had the highest specific heat; but there was no apparent correlation between the
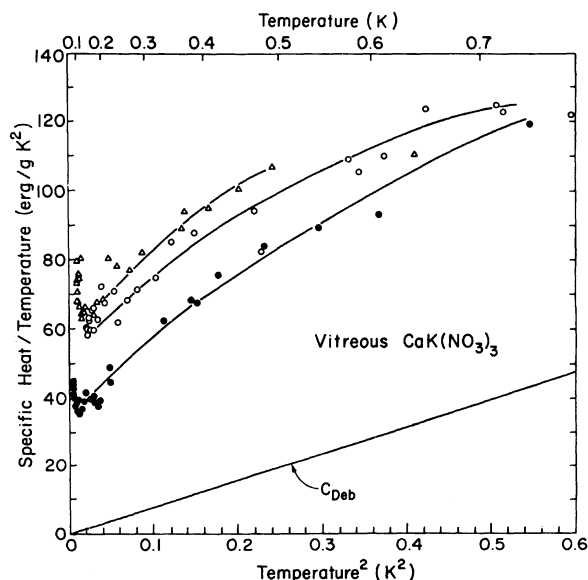
FIG. 6. Specific heat of three samples of $CaK(NO_3)_3$ plotted as C/T vs T^2. The open points are data from "wet" samples ($\triangle$ for No. 1 and o for No. 2), which contained a large amount of water of hydration. The solid points are data from the dry sample (No. 3). The line marked C_{Deb} is the heat capacity predicted by the Debye model using the speeds of sound, v_l and v_t, measured for the "dry" sample (Table I).
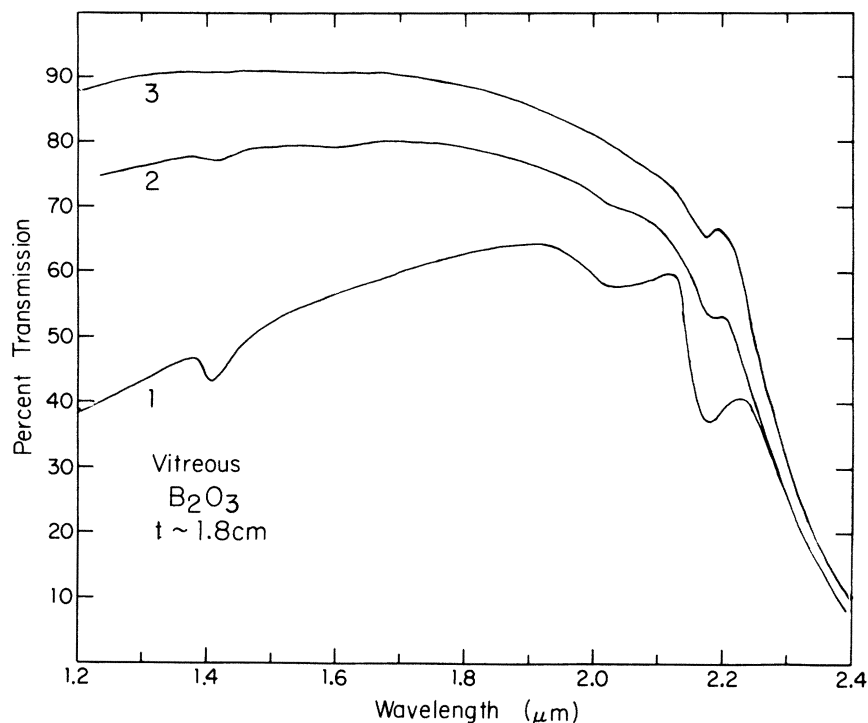
FIG. 7. Infrared absorption spectrum of B_2O_3 sample Nos. 1, 2, and 3 (see text for description of preparation). Their thicknesses are 1.78, 1.92, and 1.77 cm, respectively. The absorption bands at 1.14, 2.03, and 2.17 μm are due to water contamination. The reduced transmission for sample No. 1 at the short wavelengths is due to scattering from bulk precipates.

specific-heat differences for the other four samples (< 30%) and their remnant hydration or other impurity concentrations (> 100%).

4. As_2S_3

The As_2S_3 measurements (Fig. 9) showed the clearest indications of extrinsic effects. There were a series of four samples measured of this compound produced with escalating amounts of care. The results are summarized in Table IV.

You can see in Fig. 9 that in this case, the excess heat capacity does roughly scale with the impurity concentrations except for sample No. 4. That sample had less than 1 ppm total impurities, and yet had an excess in the heat capacity corresponding to considerably more [it is at least 5 ppm; the minimum number needed to produce the excess heat capacity is obtained by integrating the excess specific heat up to 1% of Θ_{Deb} using $S = \int (C/T)dt = Nk \ln 2$].

TABLE III. The starting material, excess specific heat, and H_2O absorption strength for different samples of B_2O_3 glass.

Sample	Prepared by	Starting Material	Max. Melt Temp. (°C)	$\int_0^1 {}^K (C_{exp} - C_{Deb}) \frac{dT^e}{T}$	H_2O absorption strength (2.17 μm) (cm^{-1})
1	Cornell	H_3BO_3 [a]	600	29(erg/g K)	0.34
2	Crystal	B_2O_3 [b]	1050	14.7	0.05
3	Growing	B_2O_3 [b]	1250	14 [f]	0.03
4	Facility	B_2O_3 [b]	1300	14.5	~0.12
5	Lasjaunias [d]	B_2O_3 [c]	1300	12.0	~0.12

[a]AR-grade H_2BO_3.

[b]Optronic grade B_2O_3 from Alfa Inorganics Inc.: $SiO_2 < 0.5$ ppm; Pb, Zn< 0.1 ppm; Cu, Fe< 0.05 ppm; otherwise > 10×purer than AR-grade material.

[c]Suprapur Boric Oxide Merck: Fe< 10 ppm, Pt< 5 ppm, Cr < 2 ppm, Co< 0.5 ppm Mn < 0.2 ppm; from Ref. 5.

[d]Data taken from Ref. 5.

[e]Based on Lasjaunias's estimate of $C_{Deb}/T^3 = 65$ erg/g K^4.

[f]After data by B. Nathan, Cornell University (unpublished).
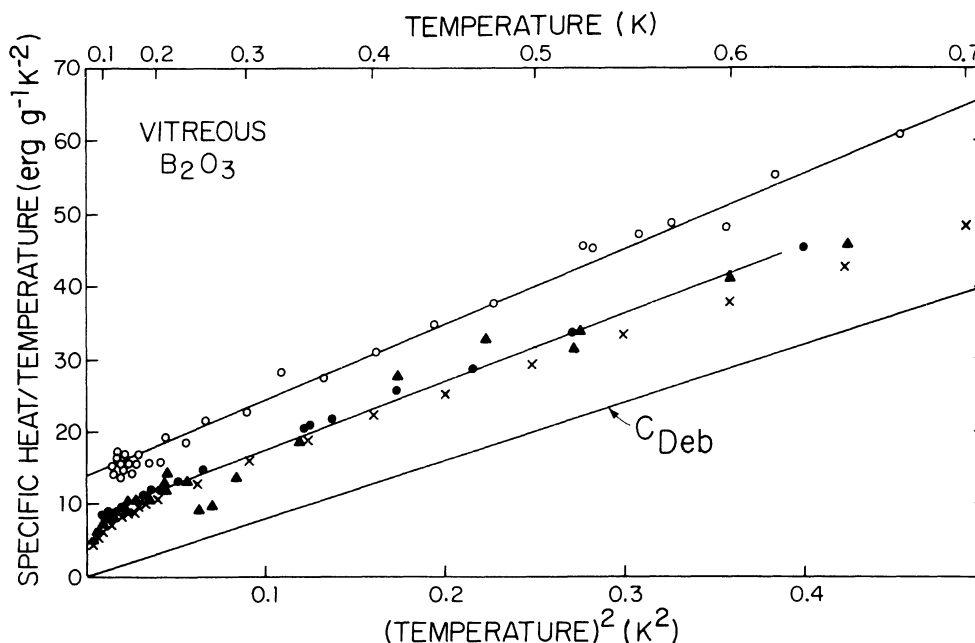
FIG. 8. Specific heat of four samples of vitreous B_2O_3 plotted as C/T vs T^2. The ×'s are after Lasjaunias *et al.*
(Ref. 6). (Sample No. 5; see Table III). The data indicated by circles are for samples measured by the author (○ for
No. 1 and ● for No. 2. Sample No. 3 (▲) was measured by B. Nathan in the same lab. See text and Table III for sample
descriptions. The line marked C_{Deb} is the heat capacity predicted by the Debye model.

It is interesting to note that all the samples pro-
duced from the hygroscopic As_2S_3 powder appear to
have a larger c_3 than the sample made from the ele-
ments As, S. It may be that in fact c_{Deb} is larger
because of water of hydration, but this proved im-
possible to check. One could neither look for H_2O
ir absorption lines or check v_{Deb}; these samples
contained large numbers of tiny bubbles (this seems
to be characteristic of samples made from the
compound[21]) and so were opaque to ir or ultrasonics
experiments.

To summarize the heat-capacity measurements
on these glasses: It proved possible to reduce the
excess heat capacity in most of these glasses by
careful preparation. Perhaps one has merely to
discover the appropriate technique for cleaning up

each glass and the remainder would disappear com-
pletely. On the other hand, the excess was never
reduced by an amount commensurate with the or-
ders-of-magnitude reduction in impurities in these
compounds. From this one could conclude that the
remaining excess heat capacity is intrinsic to the
glassy state and in some way related to the glassy
thermal properties discussed in Sec. III B. This
possibility will be examined further in Sec. III C.

In order to compactly describe the heat capaci-
ties, they have been fit with a power series

$$C = \sum_n c_n T^n \, , \tag{3}$$

where only c_1 and c_3 were necessary to achieve a
reasonable fit ($\pm 10\%$) for $0.1 < T < 1$ K. These co-

TABLE IV. Impurities in different samples of amorphous As_2S_3.

Sample	Produced by	From	Major contaminants	Analysis technique
1	Author		< 1%Sb, <100–ppm Rb	Spark source
2	Author	As_2S_3 powder	{<100 ppm Rb, <10 ppm K, Ca, Cl, Cd	Mass spectrographic
3	Harwell Labs[a]		<100 ppm Ge	analysis
4	F. J. DiSalvo	As, S	<1 ppm Fe	reported by DiSalvo

[a]Kindly provided by A. J. Leadbetter.
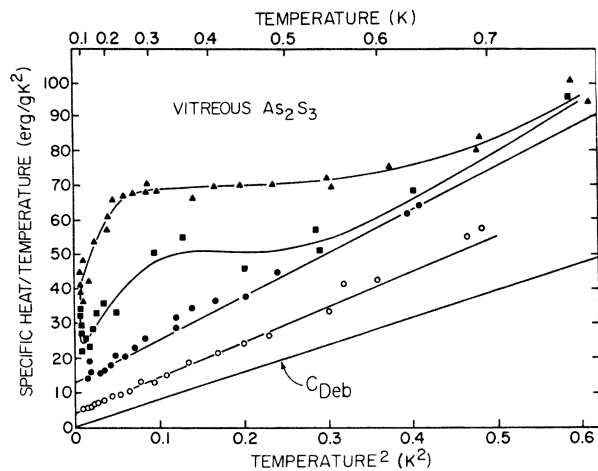
FIG. 9. Specific heat of four As_2S_3 samples plotted as C/T vs T^2. The line marked C_{Deb} is the heat capacity predicted by the Debye model. The two upper curves are from samples produced by the author with successively more care to remove water of hydration (Samples No. 1 and No. 2, respectively). The next curve is from a sample (No. 3) kindly supplied by A. J. Leadbetter, and produced by Harwell. The lowest set of data is from an ultrapure sample which was made by F. J. DiSalvo at Bell Labs. If one assumes that the differences between the upper three and lowest sets of data are due to the presence of two-level systems, one can calculate the density of these systems to be 68×10^{16} cm^{-3} for the upper curve, 26×10^{16} cm^{-3} for the second one, and 10^{16} cm^{-3} for the third. Spark-source mass spectrographic analysis of the four measured samples showed the following impurity concentrations in the order given above: (i) $< 10^{20}$ cm^{-3} Sb and $< 10^{18}$ cm^{-3} Rb; (ii) $< 10^{18}$ cm^{-3} Rb and $< 10^{17}$ cm^{-3} Cd; (iii) $< 10^{18}$ cm^{-3} Ge; (iv) nothing detectable.

efficients were worked out for the lowest observed heat capacity for each of the glasses; they are listed in Table V, columns 7 and 8. It should be stressed that there is nothing fundamental in the representation which was chosen. The simple fit used is merely descriptive, and is rarely functionally correct as one can see in Figs. 6, 8, and 10. In fact, for B_2O_3 and SiO_2 Lasjaunias[5-7] has found that to include his lower-temperature data (0.05 $< T < 0.7$ K), it is necessary to use the series

$$C = c_n T^n + c_{Deb} T^3 , \qquad (4)$$

where $n = 1.45$ for B_2O_3 and $n = 1.2 - 1.3$ for SiO_2. In contrast, Cieloszyk[3] uses the power series

$$C = c_1 T + c_2 T^2 + c_{Deb} T^3 , \qquad (5)$$

which more closely fits the data on the organic polymers which he measured. Equation (3), however, is the best form for materials like Se (Ref. 5) and As_2S_3, and the oxide glass alloys measured by Bohn.[22]

B. Thermal conductivity

If the states seen in specific-heat measurements are also responsible for the phonon scattering in glasses, we would also expect the thermal conductivity to show some sample dependence. Thermal-conductivity measurements were made of three pairs (pure and impure) of samples: As_2S_3, sample Nos. 3 and 4 (see Sec. III A); B_2O_3, sample Nos. 1 and 2; and $CaK(NO_3)_3$, sample Nos. 1 and 3. In all cases, the specific heats of these pairs of samples were significantly different. There was a factor of 2 between the As_2S_3 samples and a factor of 1.5 between the B_2O_3 and the $CaK(NO_3)_3$ samples. The thermal conductivity, however, showed no variation at all. One can see in Fig. 11 that in all three cases, the conductivity of the pure and impure samples is the same to within the experimental accuracy. For As_2S_3, the measured conductivities actually do differ by $\sim 15\%$. Note, however, that an independent measurement by Leadbetter[23] of the less pure As_2S_3 sample No. 3 resulted in data which agree with our measurements on the pure sample. Consequently, we believe that
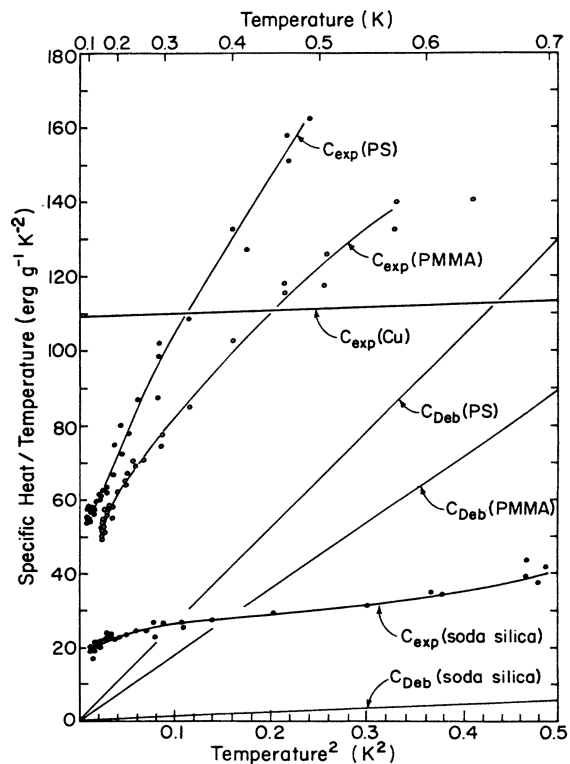
FIG. 10. Specific heat of three noncrystalline solids plotted as C/T vs T^2: $3 SiO_2 \cdot Na_2O$ (soda silica), Polystyrene (PS), and Polymethylmethacrylate (PMMA). The specific heat predicted by the Debye model, the lines marked C_{Deb}, are shown for each of the materials. The specific heat of Cu is shown for a comparison of its electronic contribution to the size of the excess $(C_{exp} - C_{Deb})$.

TABLE V. Summary of data available on low-temperature specific heat and thermal conductivity of noncrystalline solids.[a] The first four columns give some general parameters of the materials studied. Columns 5 and 6 pertain to the Debye model; the Debye temperature in column 5 is based on the atomic (not the molecular) number density. Columns 7 and 8 contain the parameters to Eq. (1) which were used to fit our specific-heat data. Note that these numbers bear very little resemblance to the coefficient c_{Deb} predicted by the Debye model (in column 6). Columns 9 and 10 are the coefficients of the equation $n(\Delta) = a + b\Delta^2$, which describes the excess density of excitations as a function of energy calculated under the assumption that they are two-level systems. The numbers one can calculate depend on the exact model used; for details see Ref. 10; n, in column 11, is the integral of these two-level states, $0.5 < T$, < 1.5 K; they are the states which would be involved in the phonon scattering at 0.3 K. Columns 12 and 13 are the parameters for the equation used to fit the thermal-conductivity data: $\Lambda = \beta(T/K)^\delta$. This equation describes the data well from $T = 0.07$ K up to 0.4–1 K (depending on the substance). Column 14 is the Debye phonon relaxation time at 0.3 K from Eq. (5); n and τ were also calculated for two atomic scatterers in KCl from data published by Narayanamurti and Pohl (Ref. 15). The numbers are given in the bottom two rows of the table.

	1	2	3	4	5	6	7	8	9	10	11	12	13	14
Material	Mass density (g/cm³)	Average atomic weight	Average molecular weight	v_{Deb} (10⁵ cm/sec)	Θ_{Deb} (K)	c_{Deb} (erg/g K⁴)	c_1 (erg/g K²)	c_3 (erg/g K⁴)	a 10³² (erg⁻¹ cm⁻²)	b 10⁶⁴ (erg⁻³ cm⁻³)	n (10¹⁶ cm⁻³)	β (10⁻⁴ W cm⁻¹ K⁻¹)	δ	τ (10⁻⁹ sec)
SiO₂-spectrosil	2.2	20	60	4.1	494	8.0	12	18	8.42	0.266	12.4	2.4	1.87	9.6
3SiO₂·Na₂O	2.4	20	61	3.51	436	11.8	21	31	16.1	0.573	23.8	1.7	1.92	5.4
Corning code No. 7740[b]	2.2	20	...	3.65	440	11.4	~10[e]	22.	7.0	0.282	10.5	2.1	1.92	6.9
Corning code No. 9700[c]	2.2	20	...	...	...	...	15.0	36.2	10.53	0.661	16.4	...	...	...
GeO₂	3.6	35	105	2.6	307	19.3	9	26	10.3	0.292	15.1	3.7	1.91	8.8
As₂S₃	3.2	49	246	1.69	171	79.0	4.4	97.7	4.5	0.725	8.26	17	1.92	24
B₂O₃	1.8	14	70	2.04	259	79.9	7.8	90.4	4.5	0.229	6.81	3.5	1.96	6.1
Se	4.3	79	79	1.19	113	170	6.6	199	9.05	1.51	16.8	7.9	1.81	8.6
Polymethyl-methacrylate	1.2	6.5	104	1.79	256	177	48	292	18.3	1.67	30.0	3.3	1.81	5.8
Polystyrene	1.0	6.7	100	1.67	223	262	53	457	16.8	2.36	30.0	2.0	1.87	3.1
Lexan[f]	1.2	7.4	238	1.53	210	284	38	410	14.5	2.12	26.1	~2	...[f]	3.8
CaK(NO₃)₃	2.1	20	217	1.94	230	79.6	39.8	148	26.7	1.74	41.8	1.6	1.90	2.9
GE No. 7031 varnish	...	...	...	...	...	...	64.5	193	...	...	...	...	...	...
Pyroceram	2.42	19.8	63.6	4.12	614	7.2	16.0	26.1[g]	...	...	...	...	...	...
KCl:Li⁺[g][h] ($T_{res} = 0.3$ K)[d]	...	...	...	...	...	...	...	...	...	...	70	...	...	...
KCl:CN⁻[h] ($T_{res} = 0.6$ K)[d]	...	...	...	...	...	...	...	...	...	...	4900	...	...	0.55

[a] Largely taken from the previous paper (Ref. 10). If one wants more information about the samples not produced for this work, or the source of the number in columns 1 to 6, see that paper. The data on the GE varnish will be published shortly [R. B. Stephens, Cryogenics 15, 420 (1975)].

[b] Nominal composition: 80.5% SiO₂, 3.8% Na₂O, 12.9% B₂O₃, 2.2% Al₂O₃, 0.4% K₂O, 0.2% Li₂O. 100 ppm Fe estimated from specific heat (Ref. 12).

[c] Nominal composition: 80% SiO₂, 13% B₂O₃, 5% Na₂O, 2% Al₂O₃. 12 ppm Fe estimated from specific heat (Ref. 12).

[d] See Ref. 15.

[e] From measurements in a 90 kG field and for $T > 1.2$ K; see R. A. Fisher, G. E. Brodale, E. W. Hornung, and W. F. Giauque, Rev. Sci. Instr. 39, 108 (1968).

[f] After Cieloszyk et al. (Ref. 2). The measurements were made down to 0.4 K; this was not low enough to determine the low temperature limit of the temperature dependence of the conductivity.

[g] A large T^2 term, $c_2 = 111$ erg/g K³ was also necessary for a good fit.

[h] In the crystals, τ is determined from the conductivity at the resonance temperature, and the effective density of states n is determined from the total number of scatterers determined chemically divided by the range in energy (temperature) over which they scatter strongly. For details, see Ref. 15, Fig. 22.
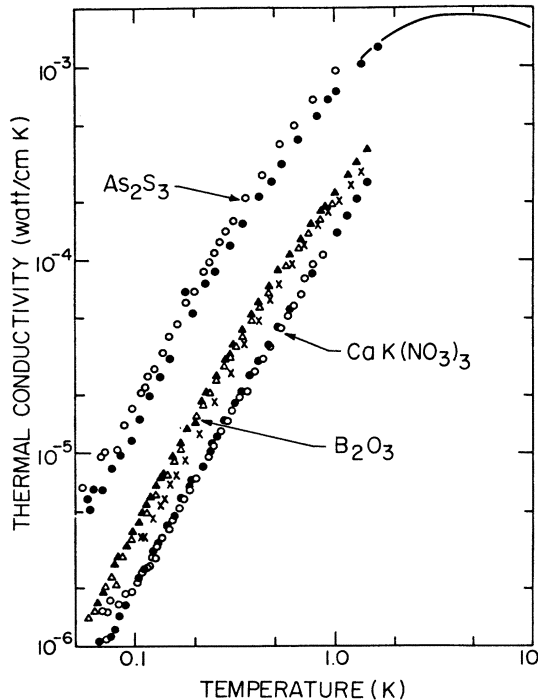
FIG. 11. Comparison of the thermal conductivity of pure and impure samples of As_2S_3, B_2O_3, and $CaK(NO_3)_3$. In all cases the data from the purer samples [As_2S_3 No. 4, B_2O_3 No. 2, and $CaK(NO_3)_3$ No. 3] are indicated with solid points, and the data from the less pure samples [As_2S_3 No. 3, B_2O_3 No. 1, and $CaK(NO_3)_3$ No. 1] are indicated with open ones. The solid line is from a measurement on As_2S_3 No. 3 by A. J. Leadbetter. The discontinuity between the two measurements on As_2S_3 No. 3 is due to a small error in calculating the l/A geometry factor for this study. If the low-temperature data were shifted to line up with Leadbetter's measurement, one can see that there would be no difference between the conductivity of the two As_2S_3 samples, just as for the B_2O_3 and $CaK(NO_3)_3$ samples. The x's are data on a B_2O_3 sample measured by Locatelli (private communication) and are lower than this study by (10–30)%. It is not known whether the sources of this difference could be due to experimental error, different temperature scale, or sample preparation.

the apparent difference between sample Nos. 1 and 3 is caused by an error in measuring the geometry factor of sample No. 3, and not by a change in the conductivity.

Lasjaunias et al.[7] have recently reported similar results for SiO_2 samples containing 1.5 and 1200 ppm OH. They found that though the samples' heat capacities differed by 50% at 0.025 K (their lowest temperature) their thermal conductivities were identical.

These observations cast a serious doubt on the previously held assumption that the excess states observed in the specific-heat measurements are related to the phonon scattering observed in ther-

mal conductivity. This question will be pursued further in Sec. III C.

C. Intrinsic excitations

All glasses have two unusual properties; an excess number of low-frequency excitations and a set of phonon scatterers. Let us, for the moment, dismiss the above arguments and pursue the idea that the excitations also scatter the phonons. One then assumes that the densities of these intrinsic excitations are actually not sample dependent; the variations in the measured specific heat are due to chemical impurities which are not strong phonon scatters. [A good example of this situation is Corning's family borosilicate glasses. Their heat capacity is increased orders of magnitude by the presence of iron (see Fig. 3) but its thermal conductivity is unaffected (see Ref. 11, Fig. 8).] We can then use the lowest observed specific heat to calculate the scattering strength for the excitations in each glass. Useful parameters for this purpose are presented in Table V along with the results of the calculations. They were done for a temperature of 0.3 K which is approximately the middle of the range of our measurements.

From the thermal conductivity, the phonon lifetime τ was calculated (Table V column 14) from the kinetic equation:

$$\Lambda(T) = \tfrac{1}{3}Cv^2\tau , \qquad (6)$$

which can be rewritten

$$\tau = 3\Lambda(T)/Cv^2 , \qquad (7)$$

where $C = c_{Deb}T^3$, $v = v_{Deb}$, and $T = 0.3$ K. It was assumed that the excess specific heat was caused by two-level systems; their density of states can be calculated from the power-series fits to the specific-heat data. At the temperature T the dominant phonons have the energy $\hbar\omega \sim 3kT$, so the two-level systems important in scattering phonons are those for which the energy-level separation Δ is given by $\Delta/k \sim 1$ K. Therefore, the number of systems n with splittings in the range of $0.5 < \Delta/k < 1.5$ K was calculated, using the lowest measured specific heat for each glass. These n's and τ's are plotted in Fig. 12. There appears to be a rough correlation between the phonon scattering rate $1/\tau$ and the number of excess states n in the different glasses. This correlation may be taken as supporting evidence for the idea that the excess specific heat and the phonon scattering are somehow related, in contrast to the observation reported in the preceding section. However, it does not imply that the mechanisms are the same.

Indeed, if one does assume that glasses' specific heat and thermal conductivity are determined by one system, it then follows that this hypothetical system is a remarkably efficient scatterer compared
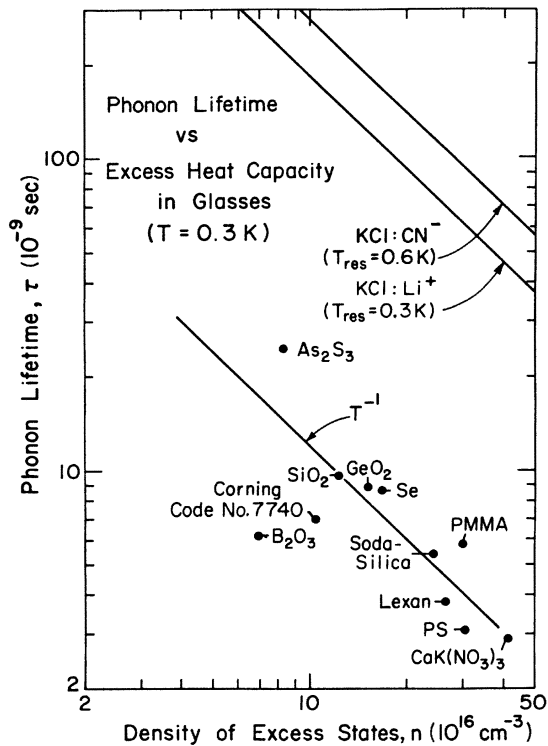
FIG. 12. Phonon lifetime vs density of excess states
at 0.3 K for all the glasses measured. The numbers
were taken from columns 11 and 14 of Table V. The
solid line is a reference T^{-1} line; that is, the relation
expected if the excess states seen in heat-capacity mea-
surements are also the dominant phonon scatterers. The
solid lines at the top are the extrapolated strengths of
CN⁻ ions and Li⁺ ions in KCL after data in Ref. 15.

to those seen in crystalline materials. If we go
through the previous calculations for tunneling sys-
tems observed in crystals, which are the strongest
phonon scatterers known in this temperature range
(CN⁻- and Li⁺-doped KCl are used for examples[24];
see Table V), we find that they are weaker than the
hypothetical glass scatterers by a factor of 10.

One may in fact have to assume even greater
scattering strengths if one tried to make the model
more realistic. In computing the values of $1/\tau$ in
Fig. 12, the assumption was made that every sys-
tem which contributed to the specific heat also
scattered phonons. This may be valid in a crys-
talline matrix, where the systems all have similar
environments and should therefore couple to the
phonons equally well, but one does not have any
assurance that those conditions are met in glasses.
In fact, the Phillips-Anderson-Halperin-Varma
tunneling model[25] expects the scattering of $3kT$
phonons to be caused by only a small fraction of
those systems which have the level separation Δ
$= 3kT$.[26] The scattering strength of these systems
then becomes so large that it is not readily ac-

ceptable without a detailed physical argument.
One such argument has been given by Lu and
Nelkin.[27] They suggested that these systems might
be arranged in one-dimensional arrays ("disloca-
tions"), so that they would scatter phonons coher-
ently, and thus much more efficiently. To date,
however, this hypothesis is not backed by any
evidence. The uncertainty should be resolved
quickly as their model makes readily testable
predictions about the form of small-angle x-ray
and light scattering in glasses. This work is pres-
ently going on at Cornell.

Our findings cast a serious doubt on a simple re-
lation between the excess specific heat and the
phonon scattering in amorphous solids. Alterna-
tively, if such a relation exists at all, such that
all or some of the states seen in the purest glasses
give rise to the observed thermal conductivity,
then these states must be very strong scatterers
relative to those known in crystals.

IV. MICROCRYSTALLINE SOLID

The uniformity of thermal properties in all the
observed glasses prompted an investigation into the
range of materials which could exhibit "glassy"
thermal properties. It is clear that perfect crys-
tals lie outside this range, but there exist many
materials whose structure is intermediate between
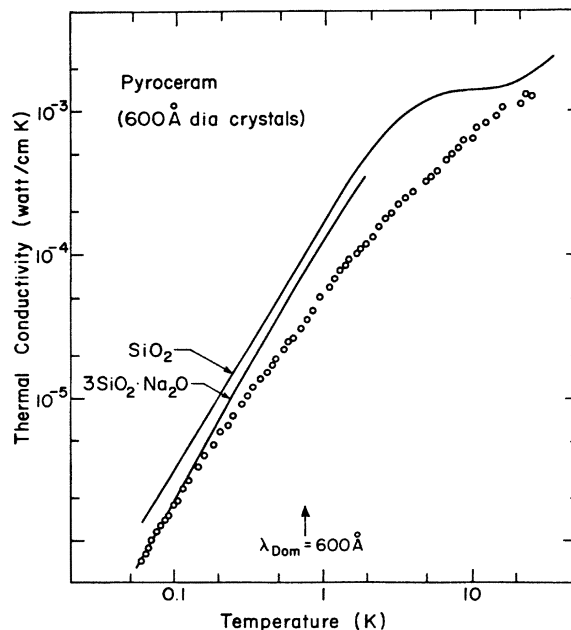
FIG. 13. Thermal conductivity vs temperature for
two samples of Pyroceram. They are both 100% crystal-
line with 600-Å-diam crystals. The very similar conduc-
tivities of soda silica glass and of vitreous silica are
shown as solid lines for comparison. The arrow at
0.8 K indicates the temperature at which the dominant
phonon wavelength is the same size as the crystals.
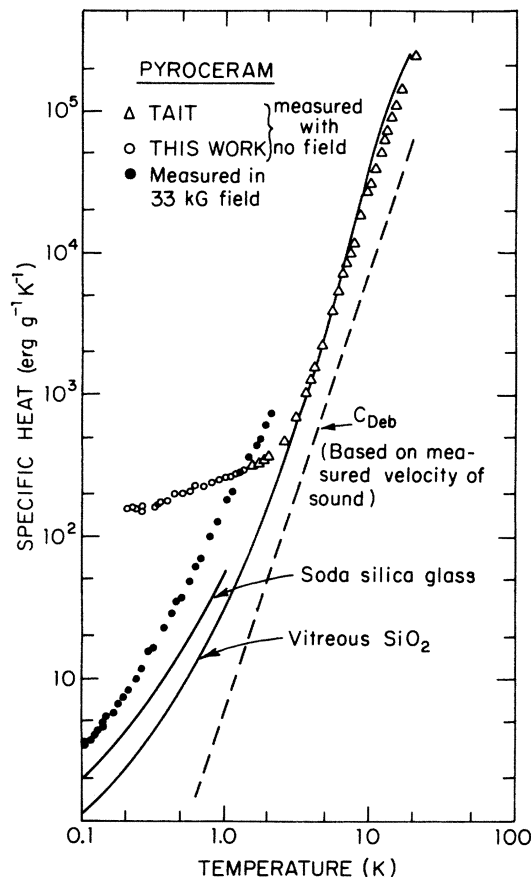
FIG. 14. Specific heat vs temperature for two samples of Pyroceram (600-Å crystals) measured in a 33-kG magnetic field (●). One was also measured in 0 kG (o). The data above 1.5 K (Δ) are after measurements by Tait (Ref. 19). The difference between the 0- and 33-kG measurements can be accounted for by about 800 ppm of iron. The magnetic field increased the splittings of the electron spin levels so that their heat-capacity contribution is shifted to higher temperatures. The field was not high enough to completely remove the electron contribution to the specific heat, so the high-field specific heat still has a substantial contribution from the spins. The specific heat of soda-silica and SIO₂ glass (which contains no spins) are shown for comparison.

the perfect long-range order of atoms in a crystal and the very short-range limit on the order observed in a glass.

Microcrystalline aggregates (ceramics, devitrified glasses, or pressed powders) are one family of such intermediate materials. Though their atoms are coherently arranged over the length of a crystalline grain, they are disordered on any larger scale. There have been thermal conductivity and specific-heat measurements on a variety of these materials above 1 K (Refs. 22 and 28) which have indicated that they have an excess in the specific heat and a markedly reduced thermal

conductivity compared to single crystals. To determine whether these characteristics are in fact similar to the glassy thermal properties, it seemed worthwhile to make similar measurements for $T < 1$ K. For this study Pyroceram, a Corning product, was chosen and preliminary measurements were made.[29]

A. Sample characterization

Pyroceram can be either glassy or polycrystalline. It was designed to have a very-low expansion coefficient when crystallized, but as a result, it is a mixture of many oxides (65% SiO_2; 23% Al_2O_3; 3.8% Li_2O; 2% ZrO_2, TiO_2; 1.8% MgO; 1.5% ZnO; 0.9% As_2O_3). The samples were kindly provided by Beall of Corning Research Lab. He reported that they had been completely crystallized to 600-Å microcrystallites. This was confirmed by electron diffraction and dark field transmission electron microscopy with a 200-keV electron microscope.

The crystals, however, are quite complex.[30] Pyroceram's major phase is a solid solution of the oxides in a β-quartz lattice (the lattice changes to a β-spodumene structure after further heat treatment). In addition, this lattice is strewn with very small ZrO_2 and TiO_2 nucleating centers.

B. Thermal conductivity

Figure 13 shows the thermal-conductivity results for crystallized Pyroceram and includes, for comparison, the conductivities of SiO_2 and $Na_2O \cdot 3SiO_2$. One can see that the thermal conductivity of the devitrified glass is rather similar to that of a typical glass. There is a substantial relative reduction centered at about 5 K and extending over $0.5 < T < 20$ K, but that can be easily understood as a result of the additional scattering caused by the interfaces between the crystallites. At the lowest temperatures, for instance, the phonon wavelengths become considerably longer than the interfacial distances ($\lambda_{Dom} = 600$ Å at 0.8 K) and so the phonons are not scattered by them. In addition to this scattering mechanism, however, another scattering mechanism is active, and this one appears to be the same as seen previously in glasses.

Even more surprising, at the highest temperatures, where the phonon wavelengths become short compared to the crystallite size and comparable to a lattice constant, one finds that the phonon mean free path is severely limited (~ 5 Å at 20 K). In spite of the crystalline appearance of these grains, as seen by electron or x-ray diffraction, there is enough disorder within them to limit the phonon mean free path as effectively as the random network of a glass. Two possible candidates for the source of this scattering could be the ZrO_2 and TiO_2 precipitates scattered throughout the crystallites.
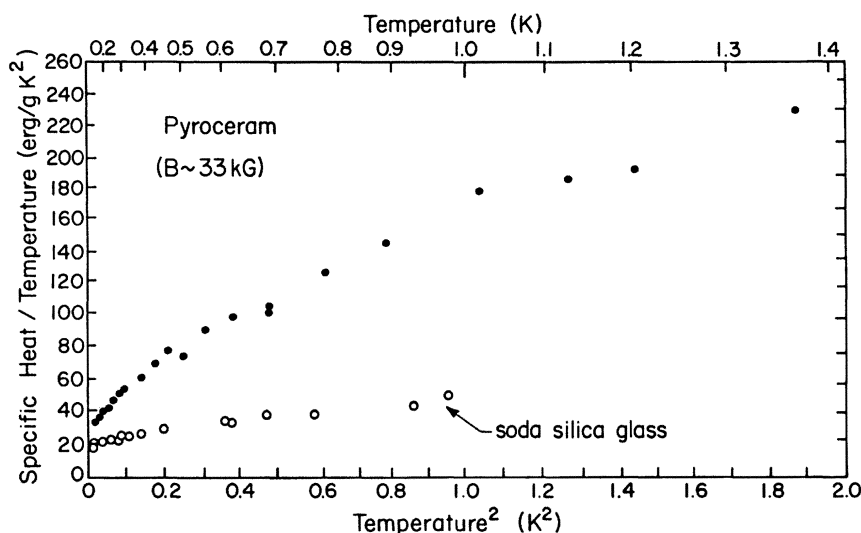
FIG. 15. Specific heat of a Pyroceram sample with 600-Å crystals in a 33-kG magnetic field. The data is plotted as C/T vs T^2. Clearly this data cannot be well fitted by a straight line ($C_{exp} = c_1 T + c_3 T^3$) and are considerably larger than other oxide glasses. The heat capacity of a soda-silica glass ($B = 0$) is shown for comparison. Most of the difference may be due to a remnant of the electron-spin contribution seen in the 0-kG measurement. With the addition of another term ($C_{exp} = c_1 T + c_2 T^2 + c_3 T^3$), the data can be fitted very well and can be extrapolated to $C/T \sim 18$ erg/gK. This is very similar to the value seen in silicate based glasses. If the electron-spin contribution dies away rapidly enough, this may in fact be the intrinsic heat capacity, but it may also be coincidental, and measurements should be redone in a higher magnetic field.

C. Specific heat

Unfortunately the specific-heat measurements were complicated by some unintentional chemical components. The first measurements (the open circles in Fig. 12) revealed that the samples had a specific heat substantially larger than that previously seen in pure glasses. It was suspected that the source of this large heat capacity was the unpaired electron spins of impurity iron ions (iron is a common contaminant in commercial silicate glasses: see Fig. 1). An attempt was made to remove this electron-spin heat capacity by applying a 33-kG magnetic field. This shifted most of the excess to higher temperatures (~ 2.2 K—you can see it in Fig. 14 as an increase in the specific heat at 33 kG for $T > 1$ K). However, due to the randomly oriented internal fields, which cause the total field to fluctuate over a wide range, there is still a significant electron-spin component to the specific heat below 1 K. (These remnant spins were not noticeable in the borosilicate measurements shown in Fig. 3 because that glass contained a factor of 80 fewer spins: ~ 800 ppm for the pyroceram versus ~ 10 ppm for the borosilicate, by chemical analysis.) In Pyroceram, the spin contribution to the specific heat is quite large and it is impossible to separate it without further experiments at higher fields than those used in this investigation. One can only observe in Fig. 15, where the data are plotted as C/T vs T^2 in order to bring out any

linear component, that in spite of the spin problems C/T extrapolates to a value similar to that of other glasses, for instance soda silica. Perhaps the spin heat capacity drops off faster than linearly with temperature and so does not affect the extrapolation, i.e., the value of 18 erg/g K^2 reflects a linear heat capacity which is intrinsic; this, however, is only a speculation and higher field measurements are necessary.

ACKNOWLEDGMENTS

[1]L. H. Challis and C. N. Hooker, J. Phys. C 5, 1153 (1972).

[2]G. S. Cieloszyk, M. T. Cruz, and G. L. Salinger, Cryogenics 13, 718 (1973).

[3]G. S. Cieloszyk, Ph.D. thesis (RPI, 1974) (unpublished).

[4]J. C. Lasjaunias, R. Maynard, and D. Thoulouse, Solid State Commun. 10, 215 (1972).

[5]J. C. Lasjaunias, Ph.D. thesis (University of Science and Medicine of Grenoble, 1973) (unpublished).

[6]J. C. Lasjaunias, D. Thoulouze, and F. Pernot, Solid State Commun. 14, 957 (1974).

[7]J. C. Lasjaunias, A. Ravex, and M. Vandorpe (unpublished).

[8]A. J. Leadbetter, Phys. Chem. Glasses 9, 1 (1968).

[9]R. B. Stephens, G. S. Cieloszyk, and G. L. Salinger, Phys. Lett. A 38, 215 (1972).

[10]R. B. Stephens, Phys. Rev. B 8, 2896 (1973).

[11]R. C. Zeller and R. O. Pohl, Phys. Rev. B 4, 2029 (1971).

[12]R. C. Zeller, M. S. thesis (Cornell University, 1971); Materials Science Center Report No. 1453 (unpublished).

[13]J. P. Harrison, Rev. Sci. Instrum. 39, 145 (1968).

[14]G. J. Sellers and A. C. Anderson, Rev. Sci. Instrum. 45, 1256 (1974).

[15]V. Narayanamurti and R. O. Pohl, Rev. Mod. Phys. 42, 201 (1970).

[16]W. H. Dumbaugh and P. C. Schultz, *Encyclopedia of Chemical Technology* (Wiley, New York, 1969), 2nd ed., Vol. 18, p. 73.

[17]G. K. White and J. A. Birch, Phys. Chem. Glasses 6, 85 (1965).

[18]J. A. Birch (private communication).

[19]P. Flubacher, A. J. Leadbetter, J. A. Morrison, and B. P. Stoicheff, J. Phys. Chem. Solids 12, 53 (1959).

[20]E. W. Hornung, R. A. Fisher, G. E. Brodale, and W. F. Giaque, J. Chem. Phys. 50, 4878 (1969).

[21]D. Henderson, Cornell University (private communication).

[22]R. G. Bohn, J. Appl. Phys. 45, 1133 (1974).

[23]A. J. Leadbetter (private communication).

[24]W. D. Seward and V. Narayanamurti, Phys. Rev. 148, 463 (1966); see also Fig. 41 of Ref. 15.

[25]W. A. Phillips, J. Low Temp. Phys. 7, 351 (1972); P. W. Anderson, B. I. Halperin, and C. M. Varma, Philos. Mag. 25, 1 (1972).

[26]J. Jäckle, Z. Phys. 257, 212 (1972).

[27]M. S. Lu and M. Nelkin, Cornell University, Materials Science Center Report No. 2415 (unpublished).

[28]W. N. Lawless, Cryogenics 15, 273 (1975); see Ref. 29 for a collection of earlier references.

[29]For a more thorough study of Pyroceram, as well as data on several other microcrystalline materials, see R. Tait, Ph.D. thesis (Cornell University, 1975) (unpublished); Materials Science Center Report No. 2452 (unpublished).

[30]G. H. Beall and D. A. Duke, J. Mater. Sci. 4, 340 (1969).